EFFECTS OF DEEP SUBSURFACE STRUCTURES ON SEISMIC WAVE PROPAGATION NEAR THE EDGE OF SEDIMENTARY PLAIN

K. Saguchi[1)], K. Motoki[2)], and K. Seo[3)]

1) *Graduate Student, Dept. of Built Environment Interdisciplinary Graduate School of Science and Engineering, Tokyo Institute of Technology, Japan*
2) *Research Associate, Dept. of Built Environment Interdisciplinary Graduate School of Science and Engineering, Tokyo Institute of Technology, Japan*
3) *Professor, Dept. of Built Environment Interdisciplinary Graduate School of Science and Engineering, Tokyo Institute of Technology, Japan*
k-sagu@enveng.titech.ac.jp, kmoto@enveng.titech.ac.jp, seo@enveng.titech.ac.jp

Abstract: Significant later phases following the S-wave arrivals in horizontal components often appear in the ground motions recorded in the sedimentary plain. In this paper, we discuss the propagation process of ground motions generated by a shallow earthquake through the analysis of seismograms recorded on rock and sediment sites. To accomplish it, we first deployed a temporary stations for seismic refraction prospecting to clear up the boundary between the mountain range and the edge of the sedimentary plain in the southwestern edge of the Kanto Plain. Accordingly, we employed the recordings of seismic waves generated by explosions to model the subsurface structures applying travel time analysis. We also applied a 2D finite difference method to simulate the later phases during an earthquake observed at the sediment sites using the subsurface structures derived from the seismic prospecting process. The results indicate that when considering basin excited waves, the characteristics of the simulated waveforms including the later phases display good agreement with the observed seismograms.

1. INTRODUCTION

It is essential to understand propagation characteristics of seismic motion in sedimentary basin in order to estimate the damage distribution from an earthquake. It has been recognized that the long-period ground motions, which consist mainly of surface waves, become larger in amplitude on sedimentary basins and longer in duration than at its margins. This is of great engineering concern. Because many large cities have a number of large-scale structures, such as high-rise buildings, long-spanned bridges and huge oil tanks in the world, including Tokyo Metropolitan area is located in a large sedimentary basin.

Tanaka et al. (1980) has reported that surface waves with a period of around 8 seconds are predominant in seismograms recorded at station on sediments in Tokyo during large earthquake. On the other hand, Toriumi et al. (1984) has pointed out that surface waves are generated secondary in the edge of basin by using seismograms from array observations. Therefore, it is necessary to consider underground structures not only particular observation sites but also process of propagation of seismic motion in order to clarify the propagation characteristics of the long-period ground motions.

In this study, seismic waves from the explosions are used to investigate the deep underground structure down to seismic basement in the Sagami area, which located at boundary between mountain region and the edge of the Kanto plain. The purpose of our investigation was to clear up the nature of the boundary between mountain region and the edge of basin, and the propagation characteristics are

discussed at this region using seismograms recorded on rock site and sediment sites due to the July 11, 2003 earthquake that occurred at the western part of Kanagawa prefecture (M=4.1,H=21km).

2. EARTHQUAKE OBSERVATION AT SOUTHWESTERN EDGE OF THE KANTO PLAIN

The southwestern part of the Kanto plain is depicted in Figure 1 with the observation points and the surface geology conditions. The Sagamihara area, located about 50km southwestern of Tokyo where is a diluvial terrace on the north side, and the Kanto Mountains, which is on the sedimentary rocks on the northwest side of this terrace.

Velocity type strong motion seismometers with three orthogonal components each were installed are 7 sites in this area. The stations ASK and AKW are located at the western part of the plain on a hard rock. YKY and FCN are located around the same area at the edge of the plain in the sediment.

Figure 2 shows an example of the horizontal components with velocity seismograms recorded at this region during the July 11, 2003 earthquake that occurred at the western part of Kanagawa prefecture (M=4.1,H=21km). Significant later phases appear following the first S-wave arrivals in horizontal components, especially transverse component at YKY and FCN. Such phenomena can be seen only in seismograms of earthquakes that occurred between the western part of Kanagawa prefecture and the eastern Yamanashi prefecture areas. The focal depth of these earthquakes is comparatively sallow (less than about 30km).

Kinoshita(1985) found seismograms observed during earthquake with the same shape from records at Fuchu array observation on the Kanto plain. As the results of analyses of characteristics of seismograms, by using apparent velocity method and Hilbert transform method. It was observed that the train of impulsive later phases was produced by multiple reflections of SH-wave at the upper boundary of dipping basement around the edge. Kurita(1996) found the significant later phase observed during the August 5, 1990 earthquake that occurred at the western part of Kanagawa prefecture (M=5.1,H=13.6km) at FCN. As the results of analyses of characteristics of seismograms, by using polarization analysis method and travel time analysis method. This phase was generated at the edge of sedimentary plain due to time difference between onset of first S-wave and first later phase. However, it has not resulted in detailed examination in propagation process because the underground structure at the edge of plain was not cleared.

3. DEEP SUBSURFACE STRUCTURES NEAR THE EDGE OF THE KANTO PLAIN

A seismic refraction prospecting was carried out in the southwestern part of the Tokyo Metropolitan area in January 15, 2000, for purpose of earthquake disaster prevention to clarify the deep underground structure down to the seismic basement. The explosions were denoted at 3 sites; Zama (SP1), Hiratsuka (SP2) and Tamagawa (SP3) are shown in Figure 3. The charge sizes were 500kg, 300kg and 50kg for SP1, SP2 and SP3, respectively.

In this experiment, we observed an explosion from SP1 by 9 stations on a 20km from Zama shot point to north observation line (N-Line), and 30 stations on a 25km east to west line (EW-Line) (Saguchi et al, 2000). EW-Line is on the line of one of the Yumenoshima explosions, of which research group made a series of seismic prospecting by exploding dynamite underground at Yumenoshima for more then twenty five times since 1975 (Research Group on Underground Structure in the Tokyo Metropolitan Area, 1989). The other group observed an explosion from SP1 by 40 stations and SP2 by 9 stations on a 15km from Zama shot point to south observation line (S-Line) along the Sagami River crossing the Hiratsuka shot point (Maeda et al, 2000). Locations of more than 70 observation stations in detail are shown in Figure 4. Digital recorders with a 200Hz sampling

recorded vertical component of ground velocity. Sensors we used geophones with a natural frequency of 4.5Hz were used for N-Line, and 2.0Hz were used for EW-Line. Synchronized time was carried out by GPS almost of stations.

Vertical component seismograms along the N-Line, the S-Line and the EW-Line released from SP1 are shown in Figure 5, respectively. The amplitudes, which were traced in Figure 5, are normalized by its maximum of each amplitude. The quality of the data is quite well and clear first arrivals corresponding to a refracted wave from seismic basement can be traced up to offsets of more than 10km along the N-Line (Figure 5(a)). The apparent P-wave velocity of the first arrivals is 5.3km/s in this section, and the intercept times are about 1.0s. On the other hand, these are not appeared along the S-Line (Figure 5 (a)), indicated that the upper layers of seismic basement are thicker than N-Line. Instead, the layer that has apparent velocity of 4.0-4.5km/s whose intercept times are about 0.5s is refracted wave from a shallow layer is recognized in both of sections. Along the S-Line, vertical component of seismic wave released from SP2 were obtained. The basin area along the EW-Line (Figure 5(b)), the apparent P-wave velocity of the first arrivals corresponding to a refracted wave from the identical layer is 3.8km/s, and the intercept times are about 0.5s. On the other hand, the mountain area crops out Cretaceous rock in this section have an apparent velocity greater than 7.0km/s. It is consider that there are interpreted as refracted wave from the seismic basement. In additionally, many later phases are recognized in all of the section. Travel time diagram for P-wave initial onsets along the line are shown in Fig. 4.Authors must follow the format details given in this section.

P-wave velocity profiles obtained from the travel time diagrams along the line are shown in Figure 6. As a primary process, the method of differences (Hagiwara, 1938) was applied to the travel time data obtained form the travel time diagrams along the S-Line, since the method is useful for understanding a general structure and also estimates approximated P-wave velocities of layer. As shown in Figure 7 (a), it consists of two layers with P-wave velocities of 2.2 and 4.3km/s from results of this method in this section. At the Zama shot point, the thickness of the upper sedimentary layer with P-wave velocity of 2.2km/s is about 0.7 km, and thinner than one at the Hiratsuka shot point. And second one with velocity of 4.3km/s. Then as a secondary process, we constructed a P-wave velocity model with three layers using by time term method along the N-Line (Figure 7 (b)) based on the result from the S-Line profile. Finally, the underground structure with a P-wave velocity along the EW-Line (Figure 7 (c)) was revealed using by time term method. It was confirmed that the basement structure of the boundary in the mountain region inclines drastically to the edge of the basin. The depth of basement in this area is about two or three hundred meters.

4. NUMERICAL SIMULATION BY FINITE-DIFFERENCE METHOD

In this study, the 2-D finite difference method is used to perform a numerical simulation. We are interested in significant later phases generation and propagation within sedimentary layers, and a observed seismogram on the rock site can be regarded as an input wave to sedimentary layers. Therefore, the velocity record of transverse component, which observed at AKW station on a hard rock, the July 11, 2003 earthquake that occurred at the western part of Kanagawa prefecture (M=4.1,H=21km), is used as input wave. The main portion of the seismogram consists of SH wave and Love waves, and set the input wave as plane wave with 45-degree incidence. It is determined by simple horizontally layered crustral structure shown in Figure 9a, which is assumed near AKW. In the computation, a band pass filter with periods from 1 to 5 second was applied considering the stable condition. This filtered record with duration of 5 second is shown in Figure 8, in which the main portion of the ground motions is included, is used as the input wave. An underground structural model for the profile along the EW-line in Figure 4 is depicted in Figure 9a, and the computed velocities on the ground surface along this line are shown Figure 9b. Three phases appear in the computed velocities, and theses phase corresponds first SH-wave, multiple reflections of SH-wave and excited

wave from the edge of plain, respectively. In this figure, it seems that the multiple reflections of SH-wave at the upper boundary of dipping basement is remarkable less than 35km from the epicenter, but excited wave which have an apparent velocity of 1.1km/s is remarkable more than 35km from the epicenter. The comparison between the observed and the synthetic seismograms at each station on the sedimentary is shown in Figure 10. According to the arrival time of each phase can be compared, it regard observed significant phases as the multiple reflections of SH-wave at the upper boundary of dipping basement at STN, YKY and FCN station. To a contrary, it turns out that the excited wave has appeared predominantly at OGM station.

5. CONCLUSIONS

The deep subsurface structure in the southwestern part of the Kanto plain was revealed by travel time analysis. The main results from our experiment are as follows the underground structure along the N-Line consists with three layers. The P-wave velocities of these layers are 2.3, 4.3 and 5.3km/s, respectively. But along the S-Line and the EW-Line, the layer with P-wave velocity of 5.3km/s was not found. Therefore, we estimate the profile along the EW-Line using by time term method based on the layer with P-wave velocity of 4.3km/s along the EW-Line. It was confirmed that the basement structure of the boundary in the mountain region inclines drastically to the edge of the plain. The depth in this area is 200 to 300 hundred meters.

We also applied a 2D finite difference method to simulate the later phases during an earthquake observed at the sediment sites using the subsurface structures derived from the seismic prospecting process. The results indicate that when considering then as basin excited waves, the characteristics of the simulated waveforms, including the later phases, display good agreement with the observed seismograms. It seems that the excited wave from edge of plain is remarkable more than 10km from the southwestern edge of the Kanto plain.

Acknowledgements:

The authors wish to express their thanks to Prof. T. Enomoto, Kanagawa Univ., Prof. N. Abeki and Mr. T. Maeda, Kanto Gakuin Univ. and Prof. K. Masaki, Aich Inst. of Tech. for making data available to the authors. They are also grateful to the public officials at Kanagawa Pref., Sagamihara City, Kawasaki City, and Yokohama City for support during this experiment. The authors would like to thank Dr. N. Yamada, Disaster Prevention Research Institute Koto University and Associate Prof. H. Yamanaka, Tokyo Inst. of Tech for making program of a finite different method available to the authors.

References:

Hagiwara, T. (1938), Travel time curve analysis for the structure with the irregular basement interface, *Zisin*, **10**, 463-468, (in Japanese).

Kinoshita, S. (1985), Propagation of total reflected phase SH pulses in a dipping layer. *Zisin*, **38**, 597-608, (in Japanese).

Maeda, T., Maeda, N. and Abeki, N. (2000), Exploration of the underground structure along the line from Zama to Hiratsuka using seismic refraction method, *Abstract of 2000 Japan Earth and Planetary Science Joint Meeting*, Tokyo, Japan, June 25-28, (in Japanese).

Neidell, N. S. and M. T. Taner (1971), Semblance and other coherency measures for multichannel data, *Geophysics*, **36**, 482-497.

Research Group on Underground Structure in the Tokyo Metropolitan Area (1989), *Technical Report on the Yumenoshima seismic refraction experiment*, Earthquake Res. Inst., University of Tokyo.

Saguchi, K., Seo, K., and Kurita, K. (2000), On the Seismic in the Southwestern Part of the Kanto Plain -Underground Structure in Sagamihara Area, Kanagawa Prefecture-, *Abstract of 2000 Japan Earth and Planetary Science Joint Meeting*, Tokyo, Japan, June 25-28, (in Japanese).

Tanaka, T., Yoshizawa, S. and Osawa, Y. (1980), Characteristics of strong earthquake ground motion in the period range from 1 to 15 seconds, *Proc. of the 7th World Conf. On Earthquake Engineering*, **vol. 2**, Istanbul, Turkey, September 8-13, 609-616.

Toriumi, I., Ohba, S. and Murai, N. (1984), Earthquake motion characteristics of Osaka plain, *Proc. of the 7th world Conf. on Earthquake Engineering*, **vol. 2**, San Francisco, California, July 21-28, 465-472.

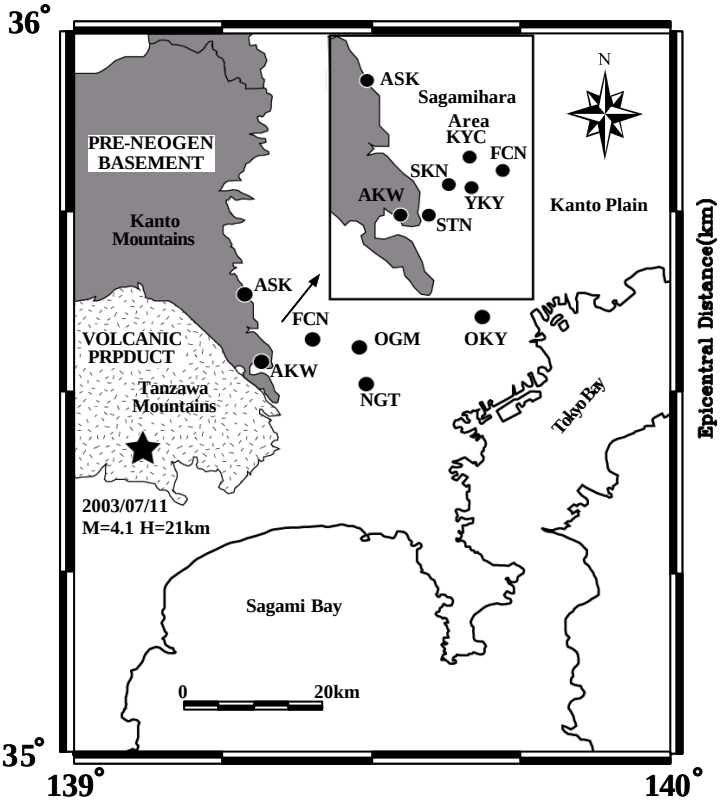

Figure 1. Map of the studied filed, the southwestern part of the Kanto plain, Japan. The solid circles indicate observation sites. The star shows the epicenter of earthquake.

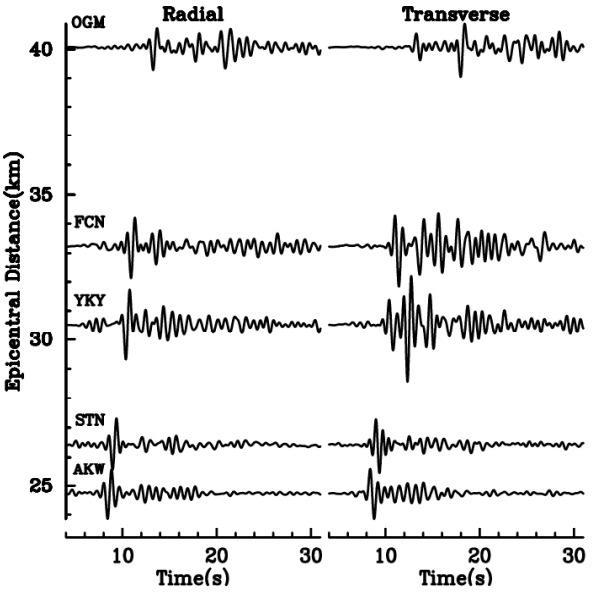

Figure 2. Horizontal velocities observed near southwestern edge of the Kanto plain during the earthquake on July, 11 in 2003. Each trace is filtered in a period range from 1 to 5 seconds.

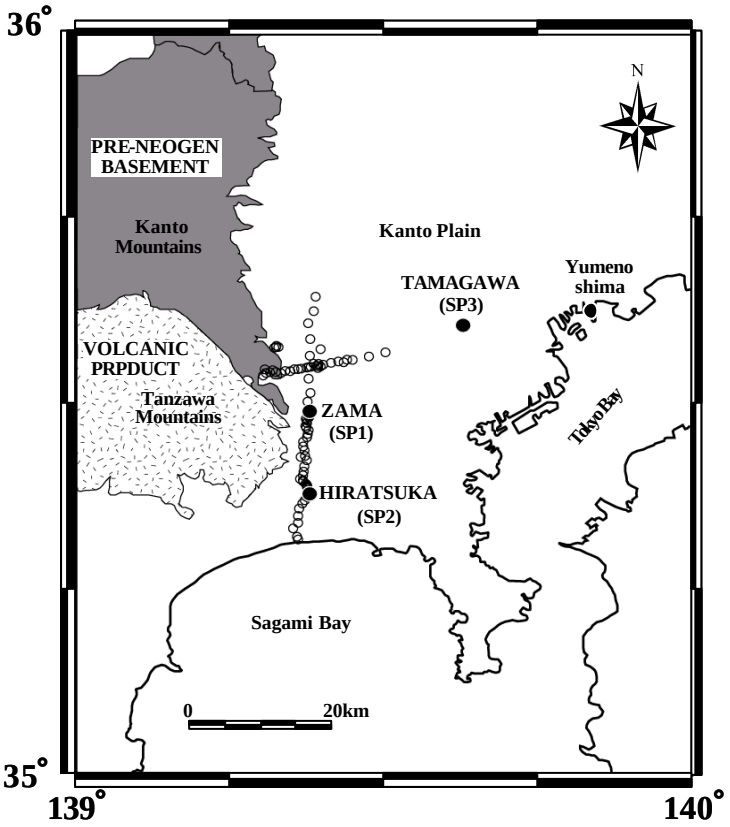

Figure 3. Map of the studied filed, the southwestern part of the Kanto plain, Japan. The solid circles and circles show explosion points and observation stations, respectively.

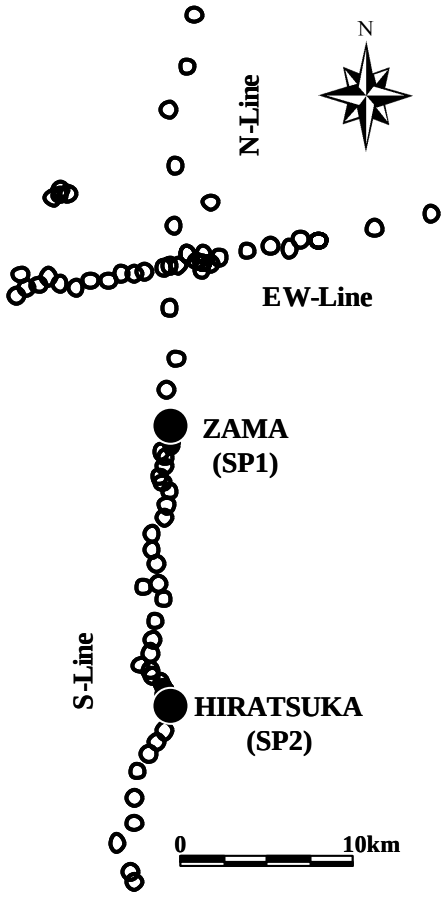

Figure 4. Map of the studied filed with the observation stations and surveying lines. N-Line located from Zama shot point to the north. S-Line located from Zama shot point to the south

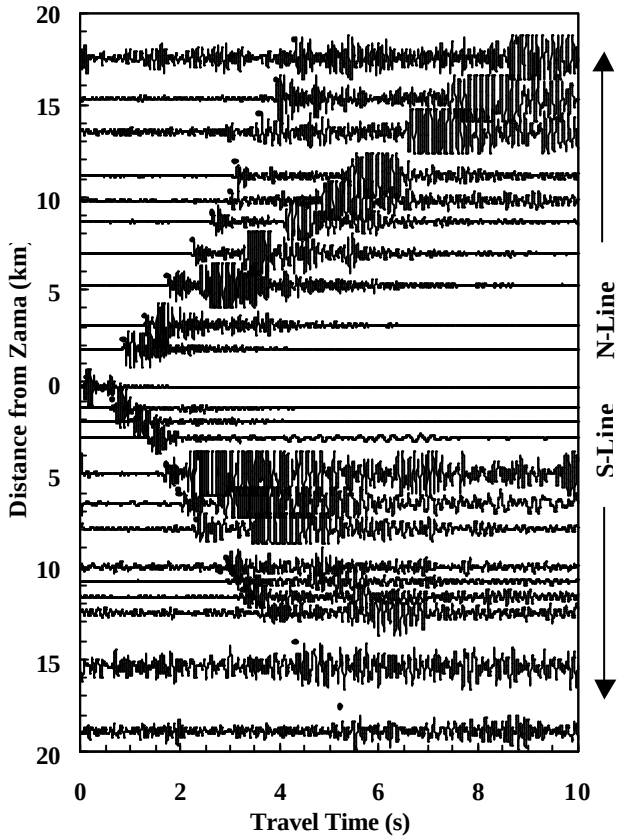

Figure 5. (a) Seismograms observed at the stations along the N-Line and the S-Line during the Zama explosion. Each trace is normalized to its maximum amplitude.

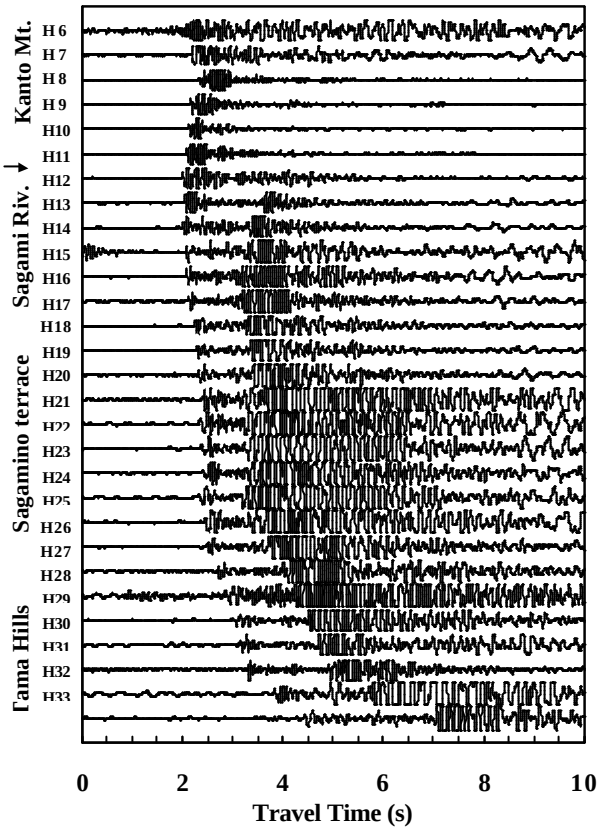

Figure 5. (b) Seismograms observed at the stations along the EW-Line during the Zama explosion. Each trace is normalized to its maximu m amplitude.

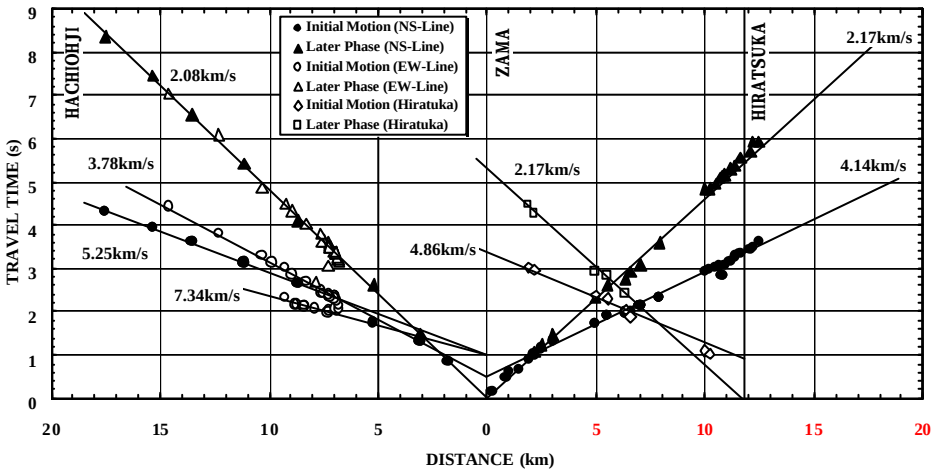

Figure 6. Travel time diagram on Hiratsuka-Hachiohji line. Solid circles and triangles show arrivals of initial and later phases for the Zama explosion, respectively. Open circles and triangles show arrivals of initial and later phases for the Zama explosion, respectively. Open squares show arrivals of initial and later phases for the Hiratsuka explosion, respectively.

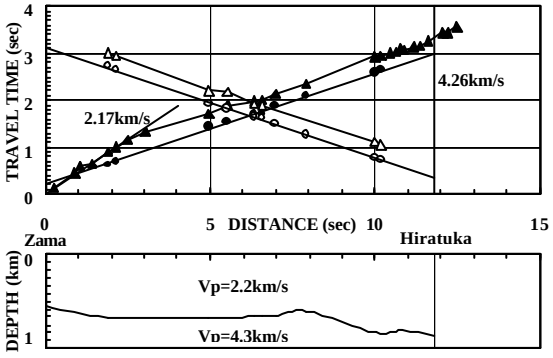

Figure 7. (a) Under ground structure obtained from the method of differences for the S-Line. Observed travel times are shown by triangles.

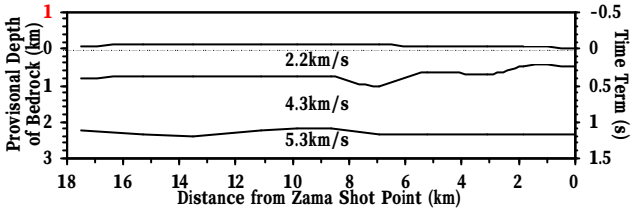

Figure 7. (b) Under ground structure obtained based on profile for the N-Line.

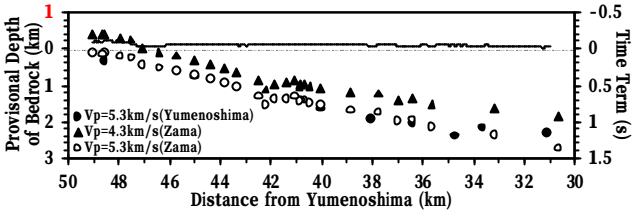

Figure 7. (c) Comparison of time terms on the EW-Line derived from Zama explosion.

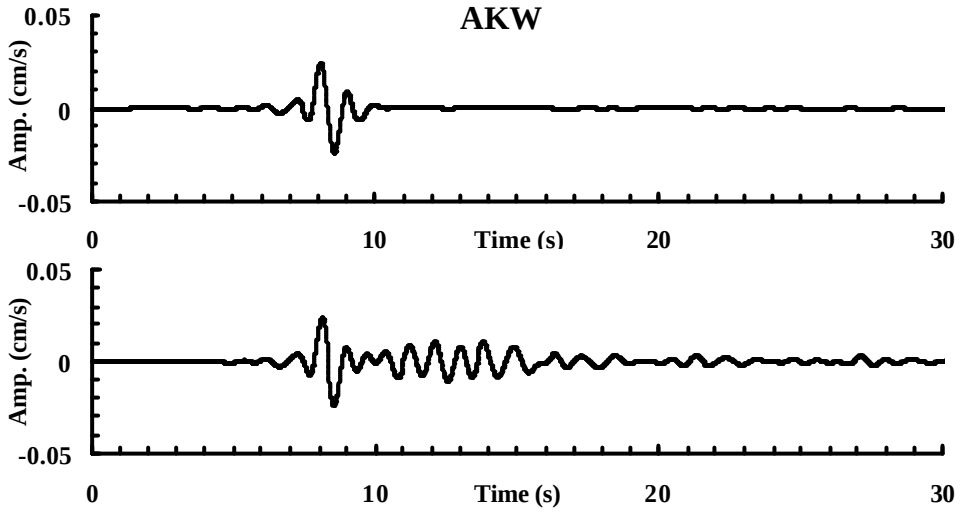

Figure 8. Input wave for calculate the waveforms using finite difference method. Upper: The only first motion observed at AKW with band pass filter in period range from 1 to 5 seconds. Lower: All data observed at AKW.

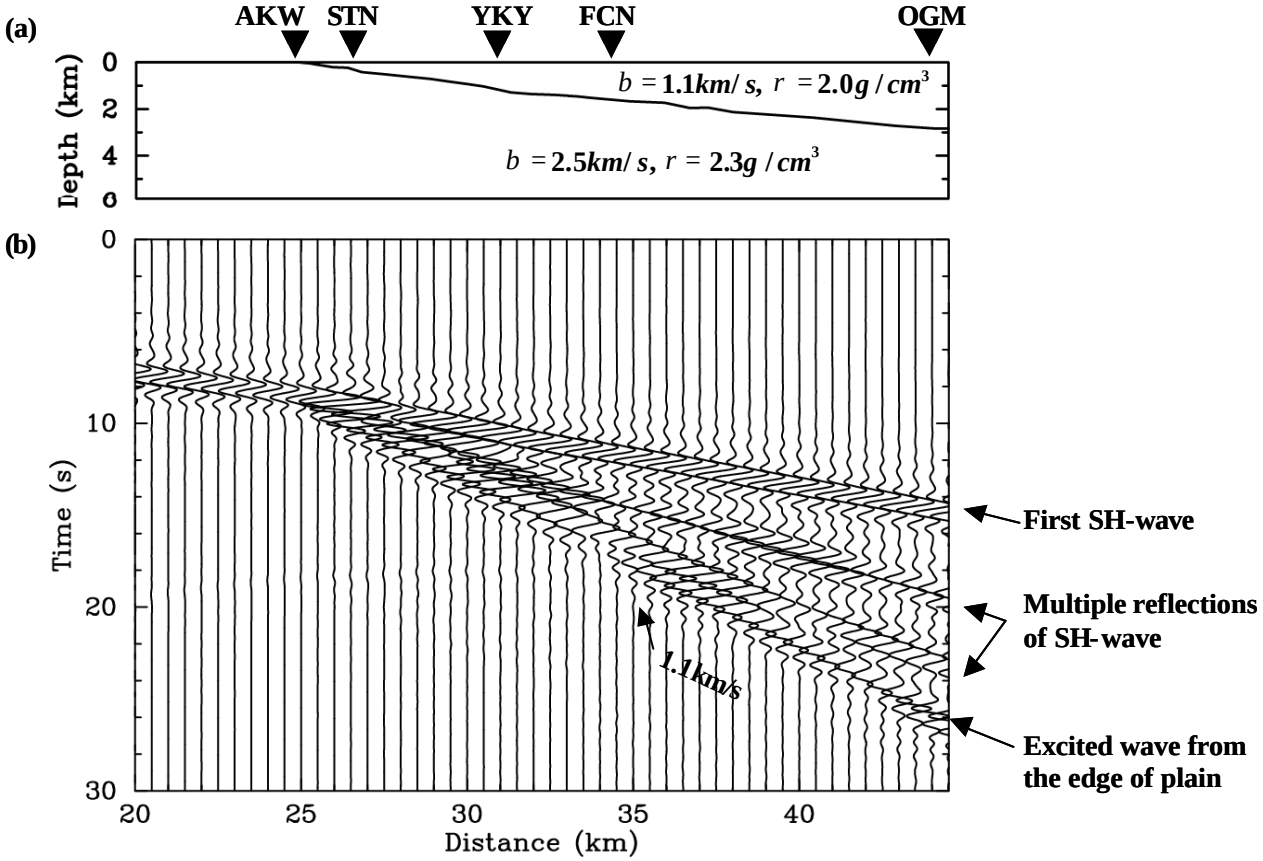

Figure 9. (a) Underground structure model along EW-line in Figure 4. (b) Synthetic velocity seismograms on the surface of the model. Each trace is normalized to maximum of all traces.

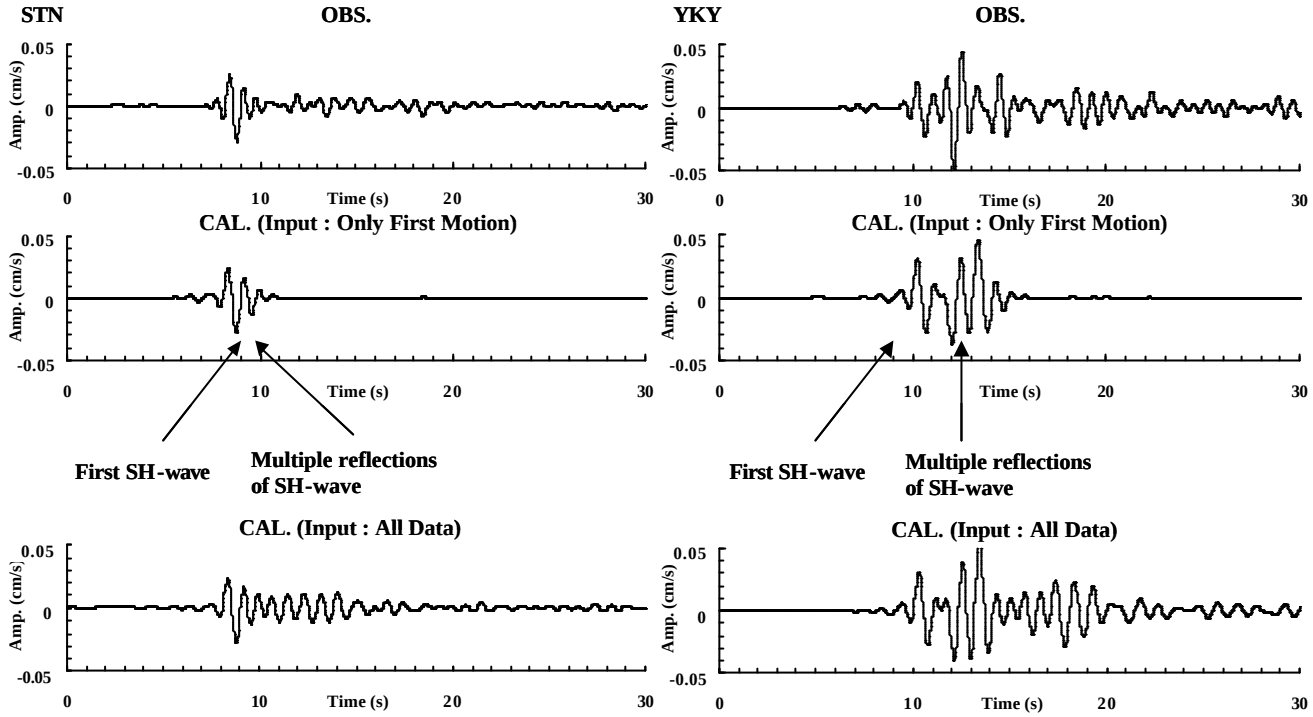

Figure 10 (a) Comparison of observed and synthetic velocities for STN (Left) and YKY (Right). Band pass filter with period from 1 to 5 seconds for the observed velocity records. Upper: Observed velocity. Middle: Synthetic velocity using the only first motion observed at AKW as an input. Lower: Synthetic velocity using all data observed at AKW as an

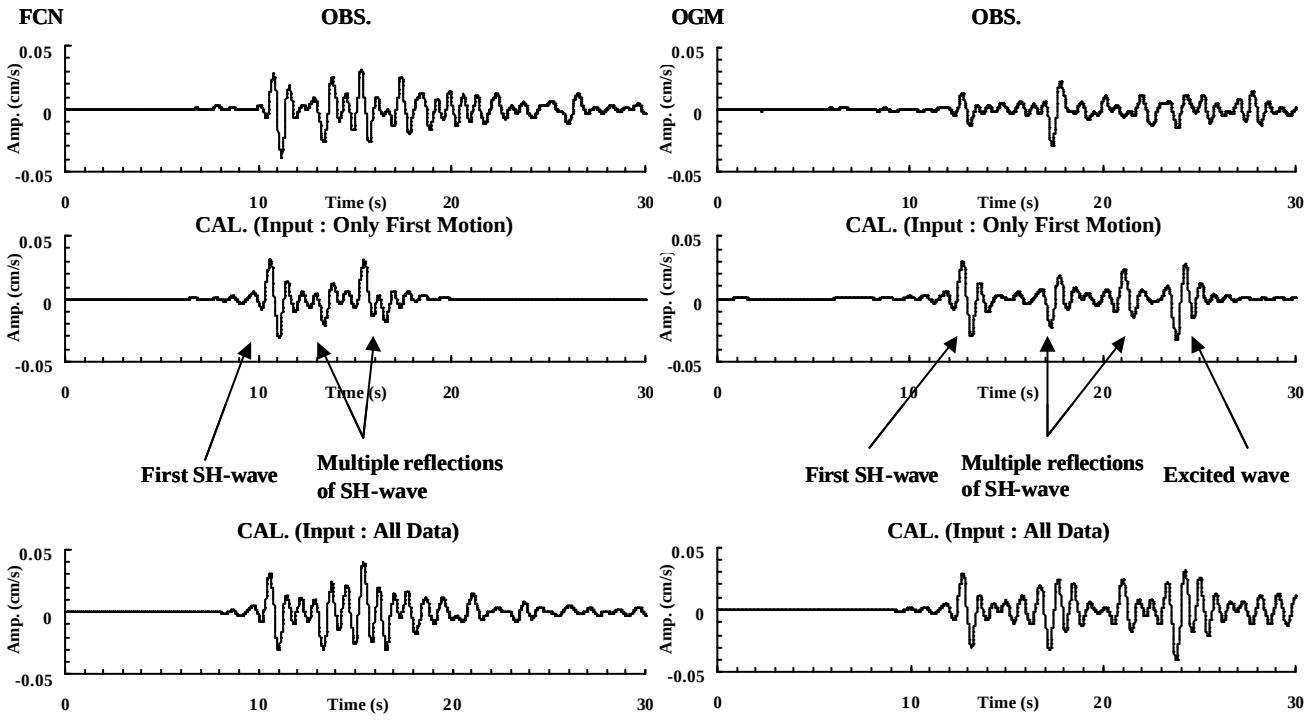

Figure 10 (b) Comparison of observed and synthetic velocities for FCN (Left) and OGM (Right). Band pass filter with period from 1 to 5 seconds for the observed velocities. Upper: Observed velocity. Middle: Synthetic velocity using the only first motion observed at AKW as an input. Lower: Synthetic velocity using all data observed at AKW as an input.